

Single-head Detonation Propagation in a Partially Obstructed Square Channel

Mark Kellenberger and Gaby Ciccarelli
Queen's University
Kingston, Ontario, Canada

1 Introduction

Understanding the mechanism of flame propagation in a channel equipped with obstacles is important for predicting the evolution of an industrial gas explosion in a congested volume. Of particular interest is the determination of the propagation mechanism of a fast-flame and detonation wave. The use of an optically accessible channel and high-speed video has provided unprecedented access to the combustion phenomena involved in these propagation regimes. The earliest study was performed by Teodorczyk et al. who showed that flame acceleration in the so-called quasi-detonation regime is characterized by repeated detonation initiation, following shock reflection off the obstacle upstream surface and channel walls, and detonation failure cycles [1]. Over the last decade, the development of megapixel high-speed digital video cameras has led to the unraveling of details of the explosion front propagation mechanism. These modern cameras are typically used as part of a schlieren optical system providing visualization of the flame and shock waves inherent to these phenomena [2]. Very recently, high-speed schlieren systems have been used in combination with soot foils [3]. The study reported in [3] showed that for a narrow channel equipped with 50% blockage fence-type obstacles mounted on the top and bottom surfaces detonation initiation at the obstacle face can lead to detonation initiation at the channel centerline. Based on all these studies, it is universally acknowledged (for medium to large blockage obstacles) that the lead shock reflection process off the obstacle upstream face governs the transition to detonation process. For obstructed channels with a square geometry, little is known of the combustion wave behaviour across the channel width. The objective of this study is to explore the three-dimensional behaviour involved in the propagation of supersonic combustion waves in an obstructed square duct.

2 Experimental

Experiments were conducted in a 3.73 m long modular aluminum combustion channel with a 7.62 cm square cross-section. Obstacles spanning the channel width and 1.91 cm in height were attached to the channel top and bottom channel walls, yielding a blockage ratio of 0.5. Obstacles were spaced one channel height apart. The channel was optically-accessible through a 44.4 cm by 7.62 cm acrylic window, located 2.46 m

downstream of the point of ignition, giving a top-down view when compared to typical studies [1, 2]. A single-pass schlieren system in conjunction with a Photron SAZ high-speed camera allowed for visualization of the combustion wave propagation. Videos were captured at up to 175,000 frames per second, while simultaneously using the soot foil technique to obtain a physical record of the quasi-detonation propagation on the channel wall. This was accomplished by lightly sooting a thin sheet of glass or aluminum with a kerosene lamp and placing it within the combustion channel. Some tests included soot-foils on multiple channel walls to determine the three-dimensional behaviour of combustion wave propagation. High-speed piezoelectric pressure transducers captured pressure-time histories at locations of 2.31 m, 2.57 m, and 3.03 m downstream of the ignition. A mixture of stoichiometric hydrogen-oxygen was used in all tests at an initial temperature of 293 K and an initial pressure of 9 - 30 kPa. The gaseous mixture was ignited from one end of the channel using an automotive capacitive discharge system.

3 Results and Discussion

Following ignition, the flame accelerates rapidly down the channel, reaching a quasi-steady velocity by the time it reaches the optical section where high-speed schlieren video and soot foils are obtained. Shown in Figure 1 is a summary of the tests conducted at different initial pressures, indicating the average velocity of the combustion wave in the optical section, based on pressure transducer time-of-arrival measurements at a given pressure. The distance between pressure transducers accommodated 7 obstacle pairs, allowing sufficient spacing for any detonation failure and reinitiation processes to occur, as is known to occur in quasi-detonation wave propagation. Also shown is the calculated equilibrium CJ detonation velocity and isobaric speed of sound of the products calculated using the chemical equilibrium code STANJAN.

There are three distinct propagation regimes that will be discussed using the aid of schlieren images and soot foil records, which will be compared to results previously obtained in a narrow channel [3]. Two of the regimes (fast flame and continuous detonation) were described in detail in [2]. The third, a single-head propagation regime, was not observed in the narrow channel and thus will be the focus of this paper. Tests performed at 9 kPa resulted in the propagation of a fast flame, see Figure 2 schlieren images, with an average velocity below the isobaric speed of sound of the combustion products. In frame 1, a shock wave interacts with obstacle 4 and a wrinkled flame front enters the field-of-view. The large distance between the shock and the flame indicates that the flame is decoupled from the shock. In Figure 2a, a Mach stem can be seen at the top and bottom channel walls behind a highly curved lead shock wave. The subsequent collision of the Mach stem with obstacle is too weak to produce a local ignition due to shock reflection. The lack of any cellular structure on soot foil records (not shown) indicate the shock velocity of approximately 1000 m/s did not initiate a DDT event. This is consistent with previous findings in [2]. Shock reflection off obstacle 4 does produce matching transverse waves (seen in frame 2) that collide at the channel centreline. Figure 2a indicates the flame tip elongates and accelerates as it contracts following the post shock flow through obstacle pair 4. The piston effect of the accelerating flame produces a secondary shock wave that can be seen in frame 5 of Figure 2a. By frame 4 it has caught up to and reinforced the lead shock wave just prior to collision with obstacle 5. Frames 5 and 6 of Figure 2a show the flame flattening as it approaches obstacle pair 5 and appears to be driven backwards in frame 6 due to the reflection of the Mach stem with the upstream obstacle face. Frame 5 of Figure 2b shows the top-view of the shock-flame interaction where a reflected wave can be seen travelling upstream, crossing the flame, while a weakened shock wave (due to diffraction around the obstacle) continues downstream. Frame 7 of Figure 2b shows a change in the large-scale flame instabilities due to both interaction with the reflected shock wave and flame acceleration due to contraction through the obstacle pair. As the flame propagates down the channel, the separation between the shock and the turbulent flame front remains large, see frame 7 of Figures 2a and 2b. While the shock and

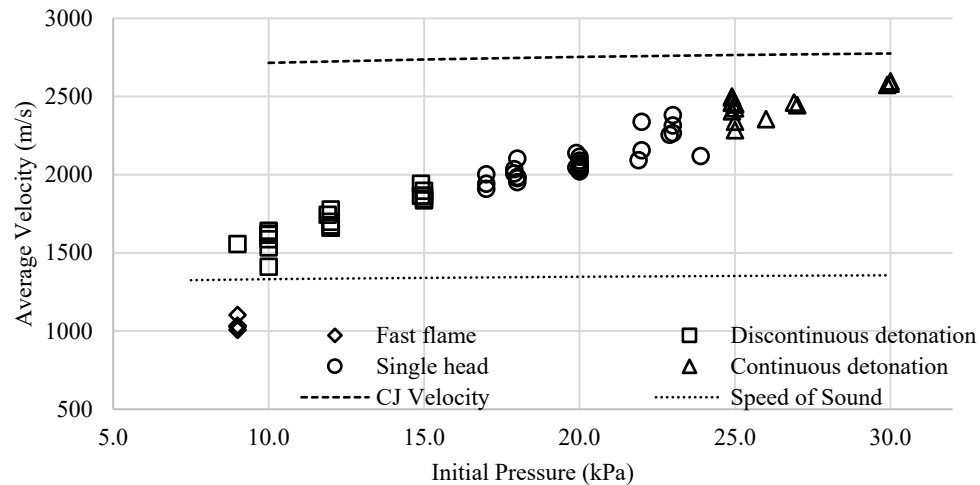


Figure 1. Average combustion wave velocity over 46 cm obtained from pressure transducer time-of-arrival. Diamond symbols represent fast flame, square symbols represent discontinuous detonation, circle symbols represent single-head detonation, triangle symbols represent continuous detonation.

flame both appear highly curved in Figure 2a, the top-view images in Figure 2b show a very planar shock. Following is a flame with large-scale corrugations, which nevertheless remains on average planar across the channel width. The large-scale corrugations are driven by flame instability resulting from both flame-shock interaction and flame acceleration driven by flow contraction through the obstacle pair. This structure is very similar to what was reported in the narrow channel [3], with the size of flame surface instabilities being qualitatively similar in the present work. This indicates that the width of the narrow channel [3] does not suppress any three-dimensional effects on fast flame propagation.

Tests at 30 kPa (shown in Figure 3) resulted in continuous detonation propagation. Frame 1 shows a shock-flame structure entering the field of view and interacting with obstacle 4. The tight coupling of the shock and flame visible in both the side and top views is indicative of the propagation of a detonation wave. The wave appears highly curved in the side-view due to diffraction around obstacle 3. As the wave interacts with obstacle 4, a strong reflection can be seen in frame 3 producing strong chemiluminescence. As the wave passes through obstacle pair 4 it flattens slightly, while the top-view indicates the detonation front remains planar across the entire channel width (frame 3 of Figure 3b) after passing over the obstacle. A thickening of the reaction zone can be seen near the top and bottom channel walls in frame 6 of Figure 3a, indicating decoupling of the detonation due to diffraction around the obstacle. The detonation wave remains coupled along the channel centreline. This is confirmed by the presence of a continuous cellular pattern on soot foils obtained from tests at an initial pressure of 30 kPa (not shown). The measured detonation velocity of 2600 m/s is only slightly higher than that obtained in the narrow channel in [2].

Tests conducted at 20 kPa yielded an average propagation velocity of approximately 2050 m/s with little scatter (see Figure 1) indicating the high repeatability of the propagation mechanism. Video frames taken from two tests at this pressure are shown in Figure 4. A curved, thick wave front enters the field-of-view in frame 1 of Figure 4a, typical of a failing detonation wave during diffraction. However, the top-view (shown in Figure 4b) reveals a much more complicated structure consisting of a highly non-planar wave with a distinct triple-point, below which is an overdriven detonation wave that extends to the bottom wall of the channel in frame 2 (the origin of this detonation wave will be described below). The appearance of

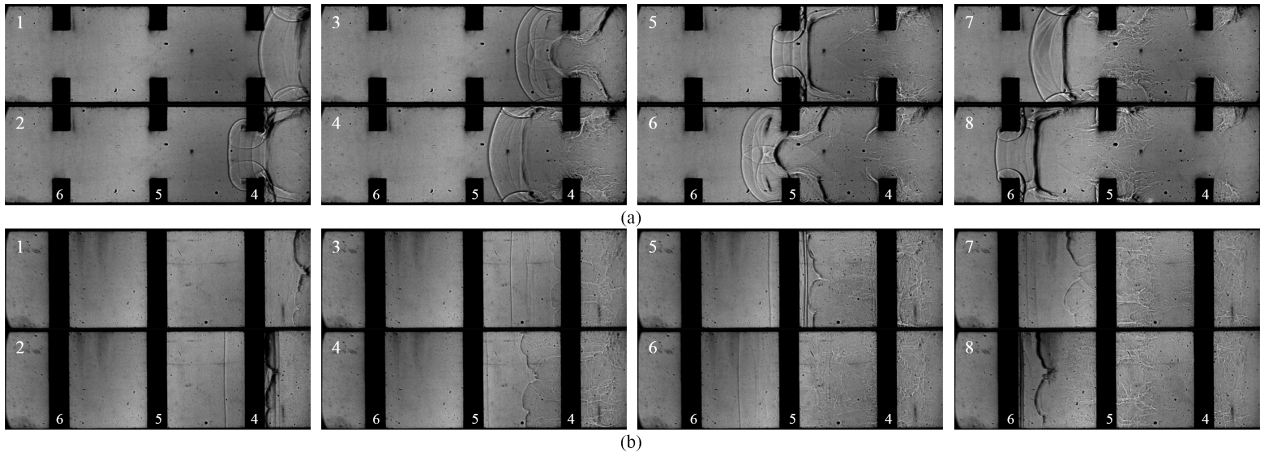


Figure 2. Schlieren image sequence of tests with stoichiometric $\text{H}_2\text{-O}_2$ at 9 kPa initial pressure (tests 201 and 165) showing fast flame propagation from (a) side-view and (b) top-view. Inter-frame time of 22.856 μs . Propagation is from right to left in frame.

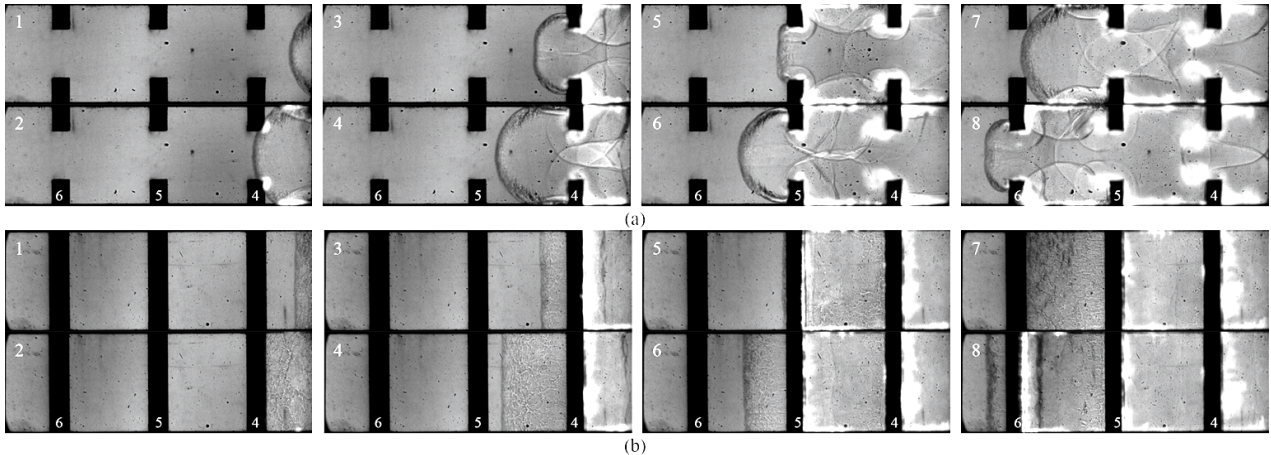


Figure 3. Schlieren image sequence of tests with stoichiometric $\text{H}_2\text{-O}_2$ at 30 kPa initial pressure (tests 201 and 176) showing continuous detonation propagation from (a) side-view and (b) top-view. Inter-frame time of 11.429 μs . Propagation is from right to left in frame.

turbulence behind the lead shock in the top-view schlieren image results from the integration effect through the highly curved surface across the channel height. Collision with obstacle 4 produces bright light at both the obstacle faces (see frames 4 and 5 in Figure 4a). The top-view images in Figure 5b shows bright light only on one end of the obstacle where the overdriven detonation reflects. The reflection of the opposite end of the wave does not produce any significant light, indicating no autoignition.

Upon passing obstacle 4, from the side-view images (Figure 4a) there appears to be two distinct fronts that persist through frames 5 to 7. The nature of this double front is revealed in the top-view images of Figure 4b. Immediately downstream of obstacle 4 in frame 6, the right half (looking downstream from the ignition end) of the front is a decoupled shock and flame, typical of a failed detonation wave. The left half of the front is typical of a curved detonation front that extends approximately halfway across the channel width to a triple-point. An overdriven detonation wave is seen to sweep transversely across the shock-compressed unburned gas region in frames 5 to 8 (see arrow in frame 6 of Figure 4b). This triple-shock configuration manifests itself as the double front seen in Figure 4a and is due to the integrating effect of the schlieren light

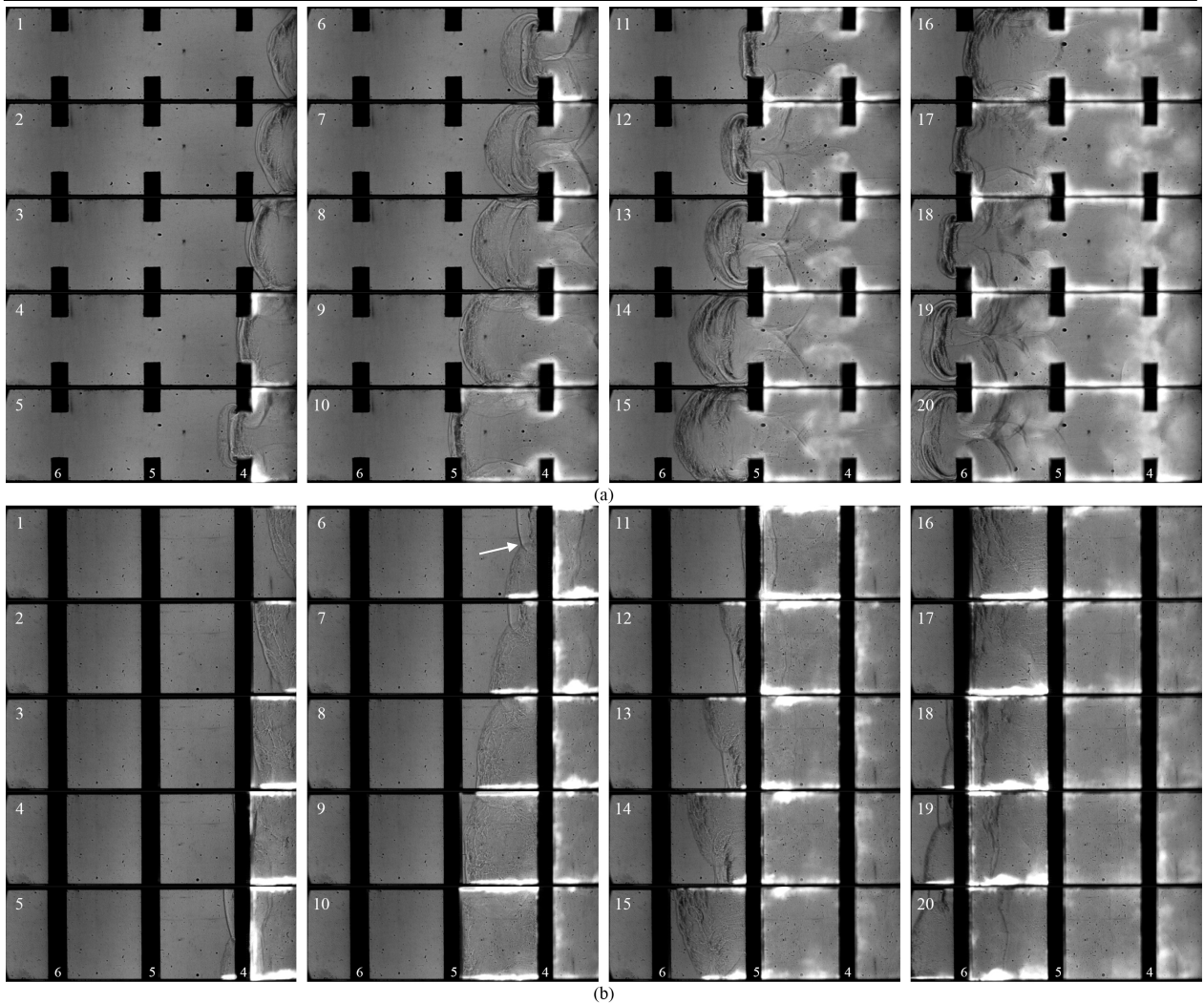


Figure 4. Schlieren image sequence of tests with stoichiometric $\text{H}_2\text{-O}_2$ at 20 kPa initial pressure (tests 177 and 191) showing single-head detonation propagation from (a) side view and (b) top view. Inter-frame time of $5.714 \mu\text{s}$. Light behind the combustion wave on the top and bottom channel surfaces is due the presence of a soot foil. Propagation is from right to left.

across the channel width. Note that it is not possible to determine from the side-view images which wall (left or right) the detonation is in contact with. The transverse overdriven detonation wave reaches the right wall just before the time of Figure 4b frame 8, at which point it produces a Mach stem detonation wave that propagates downstream along the right wall. During this time (frames 6 to 8) the detonation wave on the left side continuously decays in strength and eventually fails as it passes through obstacle pair 5, as seen in frames 12 and 13. When the Mach stem detonation propagating on the right side emerges after obstacle 5, it has grown in length due to the collision with the right wall. A new transverse overdriven detonation wave propagates towards the left wall. This transverse wave generation repeats after each obstacle pair, alternating in the direction of propagation.

The soot foil technique was used to differentiate the combustion waves on the two side walls, which is integrated in the side-view schlieren images. Soot foils were placed in the channel on the right and left walls, typical foils are shown in Figure 5. As the transverse detonation wave reaches the right wall of the channel

in frame 8 of Figure 4b, the overdriven detonation reflects. This interaction manifests itself on the soot foil as a vertical band of fine cells (see arrow), shown between obstacles 4 and 5 on the soot foil in Figure 5a. The width and location of the band correlates with the separation distance between (and position of) the decoupled shock and the trailing flame on that wall. After reflecting off the wall, the transverse detonation wave in essence continues down the wall as an overdriven detonating Mach stem that decays in strength. This produces a fine cell structure immediately after the vertical band and the cell size grows with propagation as the detonation decays in strength. Eventually the detonation decouples as it diffracts past the obstacle, producing a characteristic flaring of the triple-point trajectories. This cellular pattern is repeated on alternating sides of the channel, as can be seen on the two foils in Figure 5. Foils placed at the base of the channel (not shown) showed no cellular structure.

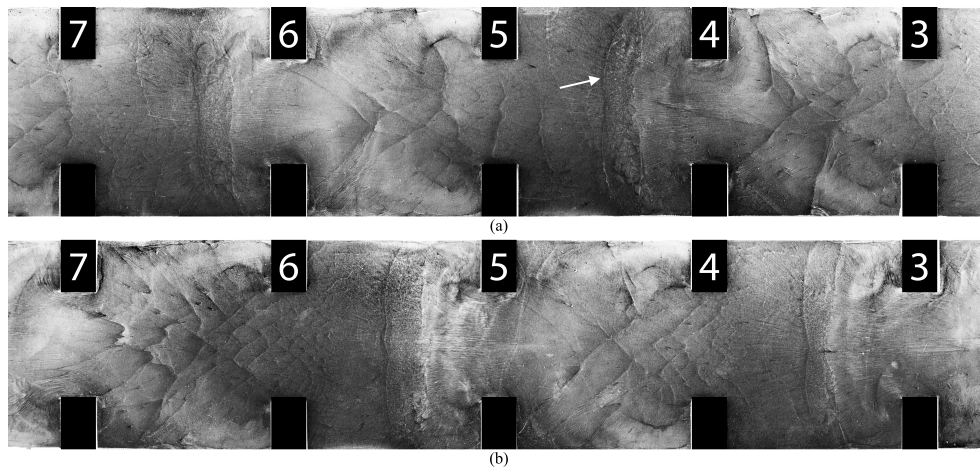


Figure 5. Soot foils from (a) right and (b) left channel walls from test in Figure 4 with stoichiometric $\text{H}_2\text{-O}_2$ at 20 kPa (test 177) showing cellular detonation pattern of single-head detonation. Propagation is from right to left.

4 Conclusions

Tests investigating the three-dimensional behaviour of propagating supersonic combustion waves were performed in an obstructed square channel. At pressures below 10 kPa, only fast flame propagation was observed, and above 25 kPa continuous detonation propagation was observed, weakening at the obstacles. Between these pressures, various forms of discontinuous detonation propagation was observed, with single-head being the most stable and reproducible in the pressure range of 17 to 23 kPa. This single-head should not be mistaken with the single-head detonation observed in an unobstructed rectangular duct [4].

References

- [1] Teodorczyk A, Lee JH, Knystautas R. (1988). Propagation mechanism of quasi-detonations. *Proc. Combust. Inst.* 22:1723-1731.
- [2] Kellenberger M, Ciccarelli G. (2015). Propagation mechanisms of supersonic combustion waves, *Proc. Combust. Inst.* 35(2):2109-2116.
- [3] Kellenberger M, Ciccarelli G. (2015). Investigation of quasi-detonation propagation using simultaneous soot foil and schlieren photography, 25th ICDERS.
- [4] Lee JHS, Soloukhin R, Oppenheim AK. (1969). Current views on gaseous detonations. *Acta Astronaut.* 14(5):537-550.